Electric Field Control of Nonvolatile Four-State Magnetization at Room Temperature

Sae Hwan Chun,[1,*] Yi Sheng Chai,[1,†] Byung-Gu Jeon,[1] Hyung Joon Kim,[1] Yoon Seok Oh,[1] Ingyu Kim,[1] Hanbit Kim,[1] Byeong Jo Jeon,[1] So Young Haam,[1] Ju-Young Park,[1] Suk Ho Lee,[1] Jae-Ho Chung,[2] Jae-Hoon Park,[3] and Kee Hoon Kim[1]

[1]*CeNSCMR, Department of Physics and Astronomy, Seoul National University, Seoul 151-747, Korea*

[2]*Department of Physics, Korea University, Seoul 136-713, Korea*

[3]*Department of Physics and Division of Advanced Materials Science, POSTECH, Pohang 790-784, Korea*

(Received 5 October 2011; revised manuscript received 23 February 2012; published 23 April 2012)

We find the realization of large converse magnetoelectric (ME) effects at room temperature in a magnetoelectric hexaferrite $Ba_{0.52}Sr_{2.48}Co_2Fe_{24}O_{41}$ single crystal, in which rapid change of electric polarization in low magnetic fields (about 5 mT) is coined to a large ME susceptibility of 3200 ps/m. The modulation of magnetization then reaches up to $0.62\mu_B$/f.u. in an electric field of 1.14 MV/m. We find further that four ME states induced by different ME poling exhibit unique, nonvolatile magnetization versus electric field curves, which can be approximately described by an effective free energy with a distinct set of ME coefficients.

DOI: 10.1103/PhysRevLett.108.177201 PACS numbers: 75.85.+t, 75.30.−m, 85.70.Ge, 85.80.Jm

The capability of the electrical control of magnetization at room temperature becomes increasingly important for many contemporary or next-generation devices such as a multibit memory [1] or a novel spintronics apparatus [2]. Multiferroics, in which magnetism and ferroelectricity coexist and couple to each other, could be the most plausible candidates to expect such a converse ME effect via their gigantic ME coupling that generally covers both linear and nonlinear effects [3–8]. Indeed, the vibrant researches on multiferroics and magnetoelectrics during the past decade have led to significant advances such as the discovery of $BiFeO_3$ with large electric polarization P [9] and numerous magnetic ferroelectrics allowing sensitive P control by a magnetic field H [3,4,10–12]. However, when the general magnetoelectric susceptibility (MES), dP/dH, is evaluated at room temperature, a $BiFeO_3$ single crystal exhibits the maximum MES of ~55 ps/m (at $\mu_0 H \leq 16$ T) [13]. Furthermore, most of the magnetic ferroelectrics indeed show the giant ME coupling far below room temperature. Although a recent discovery of the room-temperature ME effect in a polycrystalline $Sr_3Co_2Fe_{24}O_{41}$ has greatly increased the operation temperature, its maximum MES of 250 ps/m [12] is still not enough to expect a significant converse effect. Moreover, even the well-known magnetoelectrics such as Cr_2O_3 [14] and $GaFeO_3$ [15] did not show substantial modulation of bulk magnetization M by an electric field E at room temperature, mainly due to their weak ME coupling strengths ($dP/dH \leq 5$ ps/m). Therefore, the large room-temperature modulation of M by E still remains as one of great challenges that should be realized in multiferroic or magnetoelectric compounds [16–18].

To overcome the long-standing challenge, we focus here the Co_2Z-type hexaferrite $(Ba, Sr)_3Co_2Fe_{24}O_{41}$, which consists of a series of tetrahedral and octahedral Fe/Co layers stacked along the c axis (||[001]) [Fig. 1(a)]. $Sr_3Co_2Fe_{24}O_{41}$ is known to have a collinear ferrimagnetic ordering below 670 K, in which the net magnetic moments in alternating large (L) and small (S) blocks are oriented parallel to the c axis but antiparallel to each other

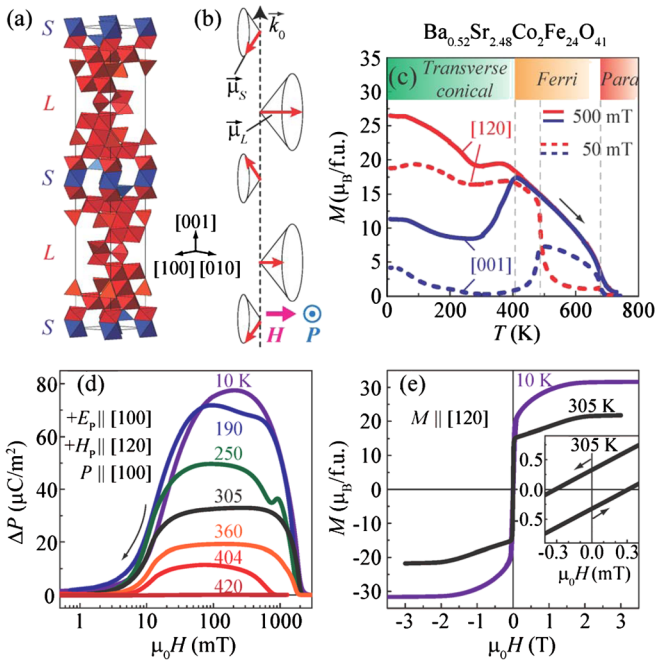

FIG. 1 (color online). (a) The Z-type hexaferrite structure in the hexagonal setting. (b) Schematic illustration of transverse conical spin states realized under a finite H. μ_L and μ_S (arrows) refer to the effective magnetic moments in the L and S blocks. (c) Temperature dependence of M||[120] and ||[001] measured at $\mu_0 H = 50$ (dashed) and 500 mT (solid) after the field cooling. (d) $\Delta P(H)(\equiv P(H) - P(H_p))$ curves after ME poling with $+\mu_0 H_p \equiv 2$ T(||[120]) and $+E_p \equiv 230$ kV/m (||[100]). (e) $M(H)$ curves at 10 and 305 K. The inset shows the magnified curve at 305 K.

($\mu_L > \mu_S$). These moments rotate away from the c axis towards the ab plane below 500 K. The ME effect appears below 400 K where a transverse conical magnetic order appears with the spin propagation vector $\vec{k}_0 = (0, 0, 1)$ [Fig. 1(b)] [19]. As the room-temperature ME effect was realized only in a polycrystalline $Sr_3Co_2Fe_{24}O_{41}$, we have then tried to grow single crystals of $(Ba, Sr)_3Co_2Fe_{24}O_{41}$ to increase the MES by either controlling directions of electric or magnetic dipoles or by tuning the chemical pressure. In this Letter, we report the successful single crystal growth of $Ba_{3-x}Sr_xCo_2Fe_{24}O_{41}$ in a broad x range. In a single crystal showing the highest MES among the series, we discover significant converse ME effects at room temperature. Furthermore, we show that the compound can save four distinct $M(E)$ curves in a nonvolatile way via independent ME writing conditions.

$Ba_{3-x}Sr_xCo_2Fe_{24}O_{41}$ ($2.40 \leq x \leq 3.00$) single crystals were grown by the flux method. Among at least four different compositions including $Sr_3Co_2Fe_{24}O_{41}$, a $Ba_{0.52}Sr_{2.48}Co_2Fe_{24}O_{41}$ single crystal showed the highest MES so that it was selected for the present study [20]. Superior to other hexaferrites [10,11,21–23], the $Ba_{0.52}Sr_{2.48}Co_2Fe_{24}O_{41}$ crystal exhibits quite high resistivity upon heat treatment [22] (2.5×10^9 Ω cm at 300 K and 1.0×10^7 Ω cm at 380 K), which allows us to measure reliably MES up to 420 K and thus to extract the corresponding $P(H)$ curves. The $M(T)$ curves measured at either $\mu_0 H = 50$ or 500 mT [Fig. 1(c)] further indicate that the ferrimagnetic order starts to develop at 680 K and magnetic easy axis changes at 490 K, followed by the stabilization of the transverse conical spin order below $T_{con} = 410$ K [20]. Our independent neutron diffraction study on the $Ba_{0.52}Sr_{2.48}Co_2Fe_{24}O_{41}$ crystal revealed the development of (0, 0, l) (l = odd) peaks below T_{con}, being consistent with the case of a polycrystalline $Sr_3Co_2Fe_{24}O_{41}$ [19]. Moreover, the neutron diffraction data could be successfully fitted by the transverse conical spin order as depicted in Fig. 1(b).

As demonstrated in Fig. 1(d), nontrivial $P(\|[100])$ is induced under a transverse H ($\|[120]$) in a wide temperature range below $T_{con} = 410$ K, yielding maximum $\Delta P(\equiv P(\mu_0 H) - P(\mu_0 H_p \equiv 2\ \mathrm{T}))$ values of 32 μC/m^2 at 305 K and 77 μC/m^2 at 10 K. Note that P rapidly increases in the 5–50 mT range, in which the magnetic hysteresis curves also show sharp, quasilinear changes [Fig. 1(e)]. This observation suggests that the spin cone axes are probably disordered in zero or small fields, whereas they are stabilized into transverse cones at $\mu_0 H \geq 50$ mT [Fig. 1(b)]. According to the spin-current model [24–26], where $\vec{P} \propto \sum \vec{k}_0 \times (\vec{\mu}_L \times \vec{\mu}_S)$ and $\vec{k}_0(\|[001])$ is the spin propagation vector, the transverse cones depicted in Fig. 1(b) allow a finite $P(\|[100])$. Therefore, alignment of the spin rotation axis toward the H direction will greatly enhance P. In a higher H region (> 1 T), in contrast, the transverse conical component will be reduced at the expense of the collinear ferrimagnetic one, eventually suppressing P. On the other hand, a magnified $M(H)$ curve at 305 K reveals a small hysteresis with a remanent $M = 0.34$ μ_B/f.u. and a small coercive field $\mu_0 H_c \approx 0.3$ mT [Fig. 1(e)], consistent with a soft ferrimagnetlike behavior in the H-controlled crossover between the disordered and ordered transverse cone states. The observation of the remanent M indicates that the transverse cone axes might not be completely disordered to contribute also to nonvanishing ΔP even in zero H bias.

Direct MES measurements with a very small ac field $\mu_0 H_{ac} = 0.02$ mT by use of a special ME susceptometer developed for detecting quite small charge oscillation down to $\sim 10^{-17}$ C [27], indeed supported the possible existence of a nonvanishing ΔP involving the remanent M. Figs. 2(a) and 2(b) show the MES data obtained after a ME poling procedure, in which H was decreased from $+\mu_0 H_p \equiv 2$ T to 1.2 T under application of $+E_p \equiv 230$ kV/m or $-E_p$ and the electric field was subsequently turned off, followed by an electrical shorting of the electrodes. Upon decreasing H from 1.2 T, the MES value for $+E_p$ increases to reach a maximum of 3200 ps/m at $\mu_0 H = 10.5$ mT, and then it decreases almost linearly

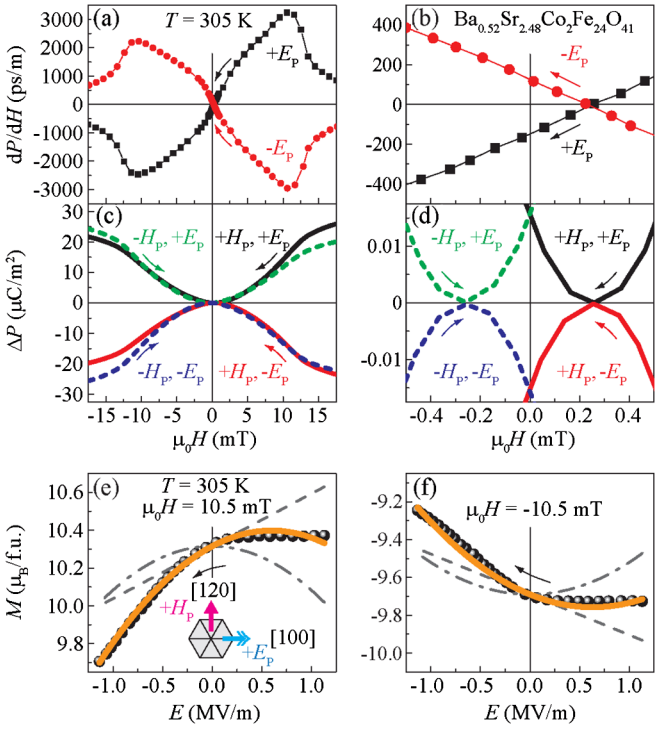

FIG. 2 (color online). (a) H dependence of MES for $+E_p$ and $-E_p$ cases at 305 K and (b) the same curve magnified near $H = 0$. (c) $\Delta P(H)$ curves and (d) the same curves enlarged near $H = 0$. Arrows indicate H-decreasing or increasing runs. (e), (f) $M(E)$ curves under bias $\mu_0 H = 10.5$ and -10.5 mT, respectively, after the ME poling with $+H_p$ and $+E_p$. Each $M(E)$ curve can be fitted with the curve (solid line) composed of linear (dashed line) and quadratic components (dash-dotted line).

to have finite intercepts in both H (0.25 mT) and dP/dH ($-$ 149 ps/m) axes [Fig. 2(b)]. Eventually it reaches a minimum of -2500 ps/m at -10.5 mT. We note that 3200 ps/m is the highest MES value ever observed in magnetoelectric or multiferroic compounds at room temperature [12–15]. Thus, the $\Delta P(H)$ curve, obtained by integrating dP/dH with H for $+E_p$, shows the steepest slope at 10.5 mT [Fig. 2(c)] and the minimum ($\Delta P_{\min} \approx 0$) at 0.25 mT [Fig. 2(d)]. At $H = 0$, we obtained a finite $\Delta P = 0.016\ \mu\text{C/m}^2$. For $-E_p$, the signs of MES as well as of ΔP are reversed to leave once again a finite $\Delta P = -0.016\ \mu\text{C/m}^2$ at $H = 0$. When the same experiment was repeated upon increasing H after the similar ME poling process starting at $-H_p$, the $\Delta P(H)$ curve consistently shows a similar sign reversal with change of electric poling direction. These observations suggest that the spin helicity, which determines the sign of the induced P according to the spin-current model, can be controlled by the electric poling direction. The finite offset in the ΔP curve at zero H-bias is likely associated with the memory effects in the spin helicity and the in-plane magnetization coming from the ME poling [28].

In order to utilize the memory effects in the M control, we first employed the ME poling ($+H_p$ and $+E_p$), termed "*state* 0", in which H was decreased from $+\mu_0 H_p \equiv 2$ T to 1.2 T under application of $+E_p \equiv 230$ kV/m and the electric field was subsequently turned off. $M(\|[120])$ was then measured at a fixed, bias $H(\|M)$ while applied $E(\|[100])$ is swept slowly in time at a frequency of 0.02 Hz. We found that M varies significantly with the E sweep in a broad H bias region below 2 T. The largest modulation was indeed observed at a bias $\mu_0 H =$ 10.5 mT, at which the MES value becomes the maximum. Figure 2(e) shows that the M modulation at 10.5 mT reaches as large as $|\Delta M \equiv M(E) - M(0)| = 0.62 \mu_B$/f.u, which corresponds to the relative change of $|\Delta M|/M(E = 0) \approx 6.0\%$. Moreover, the modulation was reproducible for many E-cycles. When the sign of H bias was reversed ($-$ 10.5 mT), we obtained somewhat reduced $|\Delta M| =$ 0.45 μ_B/f.u. and $|\Delta M|/M(E = 0) \approx 4.6\%$ [Fig. 2(f)]. These results are consistent with the smaller absolute MES value at the negative H region. In addition, as a natural consequence of the high resistivity in this system, the applied E does not generate any significant leakage current, and thus its M modulation brings only extremely small energy dissipation. Therefore, the current result demonstrates nondissipative, repeatable large M control by E at room temperature, significantly larger than the highest repeatable modulation known to date at 15 K ($|\Delta M| < 3 \times 10^{-3}\ \mu_B$/f.u) [16].

The converse ME effect could be further controlled by ME poling and H bias conditions. The $M(E)$ curves shown in Figs. 2(e) and 2(f) indeed show asymmetric line shapes, which can be decomposed into linear and quadratic terms of E that are strongly dependent upon the value of H bias. For the bias $\mu_0 H = 10.5$ mT ($-$ 10.5 mT), the $M(E)$ curve shows a positive (negative) linear slope and a negative (positive) quadratic curvature. Remarkably, we found that such asymmetric M modulation is sustained even without the H bias after the initial ME poling. The $M(E)$ curve obtained after applying the "*state* 0" [Fig. 3] shows a larger M modulation in a negative E region except for a hysteresis near zero E, thereby giving a characteristic, asymmetric parabola shape. We note that the asymmetric line shape was always reproducible regardless of the small hysteresis, which was slightly dependent on the ME poling history [20]. When the ME poling is changed into $+H_p$ & $-E_p$ (*state* 1), the $M(E)$ curve exhibits clearly different parabola shape with a larger M modulation in a positive E region. When the same experiment was repeated with $-H_p$ & $+E_p$ (*state* 2) or $-H_p$ & $-E_p$ (*state* 3), in which H was decreased from $-\mu_0 H_p \equiv -2$ T to -1.2 T under application of $+E_p \equiv 230$ kV/m or $-E_p$ and the electric field was subsequently turned off, the $M(E)$ loops display their own characteristic line shapes, distinguished from the loops for the *state* 0 or 1. As the result, the four ME poling conditions produce distinct four $M(E)$ loops. Moreover, we also found that all the $M(E)$ loops are persistently repeatable for many E cycles, proving that the ME information is nonvolatile and cannot be erased by the application of E [20]. These results suggest a unique opportunity to store nonvolatile, two-bit information in this single crystal; not only can these four states be written but they can also be read by the independent, four M values under a small E bias. Moreover, under finite $\pm E$ biases, each asymmetric $M(E)$ curve displays two independent M values. This observation also suggests yet another possibility to store eight

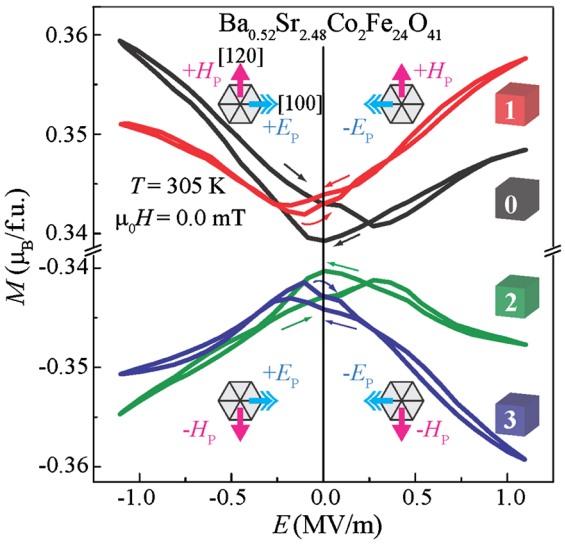

FIG. 3 (color online). The $M(E)$ curves at zero H bias obtained after applying four different ME poling (*states* 0, 1, 2, and 3) as indicated in the inset.

different states of M or four-bit information into this material under a finite E.

The $M(E)$ curves in a low H bias suggest that each curve can be effectively described by a free energy $F(E, H)$ [15],

$$F(E,H) = -PE - \mu_0 MH + \tfrac{1}{2}\varepsilon_0\varepsilon E^2 + \tfrac{1}{2}\mu_0\mu H^2 + \alpha EH + \tfrac{1}{2}\beta EH^2 + \gamma E^2 H + \tfrac{1}{2}\pi E^2 H^2 + \ldots \quad (1)$$

where ε and μ (ε_0 and μ_0) are dielectric permittivity and magnetic permeability of a material (vacuum) and α, β, γ, and π are the linear and higher order ME coefficients. By minimizing F with respect to H, the modulations of M with E and H can be described as

$$\mu_0\Delta M(E,H) \equiv \mu_0\{M(E,H) - M(0,H)\} = (\alpha + \beta H)E + (\gamma + \pi H)E^2 + \ldots \quad (2)$$

which indicates that the derived $\Delta M(E, H)$ can be approximated by a sum of linear and quadratic E terms in a low E region, being consistent with observations of an asymmetric line shape in the $M(E)$ curves [Figs. 2 and 3]. Equation (2) further suggests that the coefficients of these linear and quadratic E terms should be linearly dependent upon the H bias. To check this for each ME state [Figs. 4(a)–4(d), we fitted experimental $\Delta M(E, H)$ vs E curves at different H biases ($|\mu_0 H| \leq 10.5$ mT) with Eq. (2).

Figures 4(e) and 4(f) summarize thus determined coefficients of linear and quadratic E terms (C_1 and C_2) vs H bias, respectively. Both coefficients are indeed approximately linear in H especially near $H = 0$, and we fitted the curves in Figs. 4(e) and 4(f) with a functional form of $\alpha + \beta H$ and $\gamma + \pi H$, respectively, to determine the ME coefficients α, β, γ, and π for each ME state. We note that the observation of nonzero α, β, γ, and π values is consistent with the expected ME coefficients in a transverse conical spin ordering, for which its magnetic point group $2'$ is expected in a finite H experiment [19,20]. We further note that the resultant ME coefficients have almost the same magnitudes but characteristic signs for different ME states. This directly proves that the written ME states can be described by a distinct set of ME coefficients. Moreover, both direct ME and converse ME effects at 305 K can appear in accordance with those stored ME states. It is further inferred that the microscopic parameters such as spin helicity, cone shape, and net spin direction can be also uniquely determined for each ME state, which is characterized by a unique set of the ME coefficients. Therefore, we expect that further understanding on the relationship between the microscopic spin configuration and those ME coefficients are likely to help optimizing the converse ME effects at room temperature.

The hysteretic behavior observed in Fig. 3 should be another important phenomena that are worthy of further investigations. We found out that the hysteretic part, albeit small, was somewhat dependent upon the history of the applied E bias and its magnitude. For example, it was reduced upon decreasing maximum E value or applying E bias down to zero H region [20]. It seems thus associated

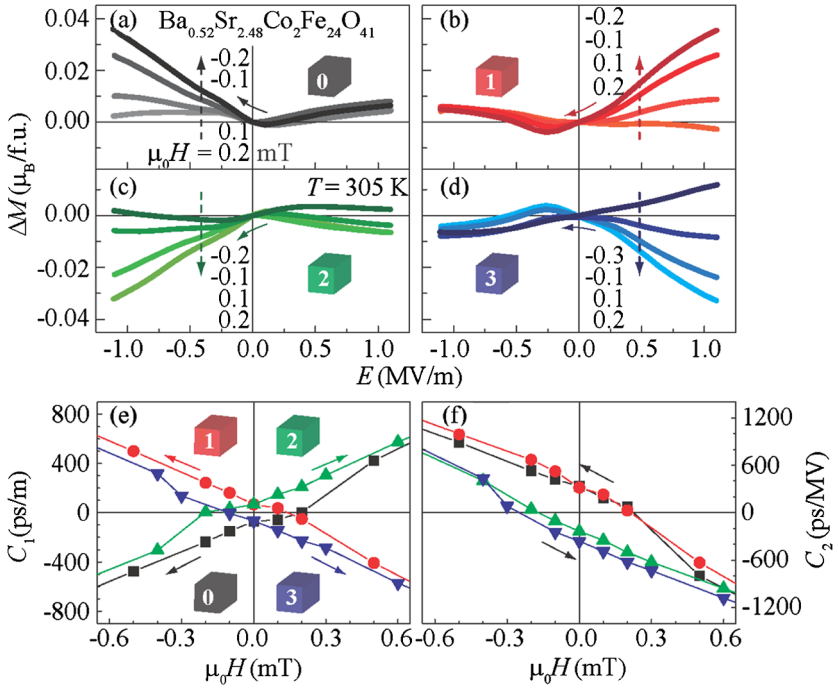

FIG. 4 (color online). (a)–(d) $\Delta M(E)$ curves under different H bias for the four different ME poling conditions (states 0–3 in Fig. 3). (e),(f) The coefficients C_1 and C_2 vs H bias for *states* 0–3 upon fitting the experimental ΔM curves in (a)–(d) with $\Delta M = C_1 E + C_2 E^2$.

with the partial switching of magnetoelectric domains under application of rather a high electric field, which can be sensitive to the history and the magnitude of the applied electric field in low H regions. Although the hysteresis turns out to be rather small in this compound, maximizing such hysteretic effects would be desirable for realizing distinct M values even without E bias.

In summary, we demonstrated the large bulk magnetization modulation by an electric field at room temperature in the hexaferrite $Ba_{0.52}Sr_{2.48}Co_2Fe_{24}O_{41}$ crystal. Four independent magnetization vs electric field curves, generated by the ME poling processes, represent four different ME states and can be described by a unique set of ME coefficients. Our result provides a proof of feasibility for utilizing the converse ME effect for a multibit memory, and thus may pave a pathway into development of a practical ME device at room temperature.

This work is supported by CRI (2010-0018300), BSR (2009-0083512) programs and the Fundamental R&D program for Core Technology of Materials. J.-H. C. is supported by the National Nuclear R&D Program of NRF (2011-0031933). J.-H. P. is supported by CRI (2009-0081576), WCU (R31-2008-000-10059-0) and LFRIR (2010-00471) programs.

*pokchun@snu.ac.kr
†hawkchai@gmail.com

[1] M. Gajek, M. Bibes, S. Fusil, K. Bouzehouane, J. Fontcuberta, A. Barthélémy, and A. Fert, Nature Mater. **6**, 296 (2007).
[2] Y.-H. Chu *et al.*, Nature Mater. **7**, 478 (2008).
[3] T. Kimura, T. Goto, H. Shintani, K. Ishizaka, T. Arima, and Y. Tokura, Nature (London) **426**, 55 (2003).
[4] N. Hur, S. Park, P. A. Sharma, J. S. Ahn, S. Guha, and S-W. Cheong, Nature (London) **429**, 392 (2004).
[5] W. Eerenstein, N. D. Mathur, and J. F. Scott, Nature (London) **442**, 759 (2006).
[6] S.-W. Cheong and M. Mostovoy, Nature Mater. **6**, 13 (2007).
[7] R. Ramesh and N. A. Spaldin, Nature Mater. **6**, 21 (2007).
[8] Y. Tokura and S. Seki, Adv. Mater. **22**, 1554 (2010).
[9] J. Wang *et al.*, Science **299**, 1719 (2003).
[10] S. Ishiwata, Y. Taguchi, H. Murakawa, Y. Onose, and Y. Tokura, Science **319**, 1643 (2008).
[11] S. H. Chun *et al.*, Phys. Rev. Lett. **104**, 037204 (2010).
[12] Y. Kitagawa, Y. Hiraoka, T. Honda, T. Ishikura, H. Nakamura, and T. Kimura, Nature Mater. **9**, 797 (2010).
[13] M. Tokunaga, M. Azuma, and Y. Shimakawa, J. Phys. Soc. Jpn. **79**, 064713 (2010).
[14] D. N. Astrov, Sov. Phys. JETP **11**, 708 (1960).
[15] G. T. Rado, Phys. Rev. Lett. **13**, 335 (1964).
[16] M. Saito, K. Ishikawa, S. Konno, K. Taniguchi, and T. Arima, Nature Mater. **8**, 634 (2009).
[17] Y. Tokunaga, N. Furukawa, H. Sakai, Y. Taguchi, T. Arima, and Y. Tokura, Nature Mater. **8**, 558 (2009).
[18] Y. J. Choi, C. L. Zhang, N. Lee, and S.-W. Cheong, Phys. Rev. Lett. **105**, 097201 (2010).
[19] M. Soda, T. Ishikura, H. Nakamura, Y. Wakabayashi, and T. Kimura, Phys. Rev. Lett. **106**, 087201 (2011).
[20] See Supplemental Material at http://link.aps.org/supplemental/10.1103/PhysRevLett.108.177201 for the sample preparation, the measurements, and the ME coefficients.
[21] T. Kimura, G. Lawes, and A. P. Ramirez, Phys. Rev. Lett. **94**, 137201 (2005).
[22] Y. S. Chai, S. H. Chun, S. Y. Haam, Y. S. Oh, I. Kim, and K. H. Kim, New J. Phys. **11**, 073030 (2009).
[23] Y. Tokunaga, Y. Kaneko, D. Okuyama, S. Ishiwata, T. Arima, S. Wakimoto, K. Kakurai, Y. Taguchi, and Y. Tokura, Phys. Rev. Lett. **105**, 257201 (2010).
[24] H. Katsura, N. Nagaosa, and A. V. Balatsky, Phys. Rev. Lett. **95**, 057205 (2005).
[25] M. Mostovoy, Phys. Rev. Lett. **96**, 067601 (2006).
[26] I. A. Sergienko and E. Dagotto, Phys. Rev. B **73**, 094434 (2006).
[27] H. Ryu *et al.*, Appl. Phys. Lett. **89**, 102907 (2006); Y. S. Oh, S. Crane, H. Zheng, Y. H. Chu, R. Ramesh, and K. H. Kim, Appl. Phys. Lett. **97**, 052902 (2010); K.-T. Ko *et al.*, Nature Commun. **2**, 567 (2011); the resolutions of MES and ΔP in our sample were estimated to be about 0.1 ps/m and 10^{-5} $\mu C/m^2$, respectively.
[28] Ferroelectricity could not be confirmed based on a $P - E$ hysteresis loop at 305 K, while the remanent ΔP still showed a sign change upon applying a post-electric field poling [20].